Video Article

Determining the Ice-binding Planes of Antifreeze Proteins by Fluorescence-based Ice Plane Affinity

Koli Basu[1], Christopher P. Garnham[2], Yoshiyuki Nishimiya[3], Sakae Tsuda[3], Ido Braslavsky[4], Peter Davies[1]

[1]Department of Biomedical and Molecular Sciences, Queen's University

[2]National Institute of Neurological Disorders and Stroke, Porter Neuroscience Research Center

[3]Research Institute of Genome-Based Biofactory, National Institute of Advanced Industrial Science and Technology

[4]The Robert H. Smith Faculty of Agriculture, Food and Environment, Institute of Biochemistry, Food Science, and Nutrition, The Hebrew University of Jerusalem

Correspondence to: Peter Davies at peter.davies@queensu.ca

URL: http://www.jove.com/video/51185
DOI: doi:10.3791/51185

Keywords: Chemistry, Issue 83, Materials, Life Sciences, Optics, antifreeze proteins, Ice adsorption, Fluorescent labeling, Ice lattice planes, ice-binding proteins, Single ice crystal

Date Published: 1/15/2014

Citation: Basu, K., Garnham, C.P., Nishimiya, Y., Tsuda, S., Braslavsky, I., Davies, P. Determining the Ice-binding Planes of Antifreeze Proteins by Fluorescence-based Ice Plane Affinity. *J. Vis. Exp.* (83), e51185, doi:10.3791/51185 (2014).

Abstract

Antifreeze proteins (AFPs) are expressed in a variety of cold-hardy organisms to prevent or slow internal ice growth. AFPs bind to specific planes of ice through their ice-binding surfaces. Fluorescence-based ice plane affinity (FIPA) analysis is a modified technique used to determine the ice planes to which the AFPs bind. FIPA is based on the original ice-etching method for determining AFP-bound ice-planes. It produces clearer images in a shortened experimental time. In FIPA analysis, AFPs are fluorescently labeled with a chimeric tag or a covalent dye then slowly incorporated into a macroscopic single ice crystal, which has been preformed into a hemisphere and oriented to determine the *a*- and *c*-axes. The AFP-bound ice hemisphere is imaged under UV light to visualize AFP-bound planes using filters to block out nonspecific light. Fluorescent labeling of the AFPs allows real-time monitoring of AFP adsorption into ice. The labels have been found not to influence the planes to which AFPs bind. FIPA analysis also introduces the option to bind more than one differently tagged AFP on the same single ice crystal to help differentiate their binding planes. These applications of FIPA are helping to advance our understanding of how AFPs bind to ice to halt its growth and why many AFP-producing organisms express multiple AFP isoforms.

Video Link

The video component of this article can be found at http://www.jove.com/video/51185/

Introduction

The production of antifreeze proteins (AFPs) is an important survival mechanism of some organisms that live in ice-laden environments. Until recently, it was thought that the sole function of AFPs was to prevent or slow the growth of internal ice crystals that would block circulation, cause tissue damage, and osmotic stress. Organisms that cannot tolerate any degree of freezing, such as fish, express AFPs to completely inhibit ice crystal growth[1]. Others, such as grass, are freeze tolerant and express AFPs to inhibit ice recrystallization which reduces the formation of large ice crystals in their tissues[2]. Stabilization of membranes in low temperature is yet another function that was suggested for the AFPs[3]. Recently, a novel role was suggested for the AFP of an Antarctic bacterium, *Marinomonas primoryensis*, from ice-covered brackish lakes[4]. This AFP is part of a much larger adhesin protein[5] that is thought to attach the bacterium to ice for better access to oxygen and nutrients[6]. Other microbes are known to secrete AFPs, which might alter the structure of the ice in which they live[7].

AFPs have been found in some fish, insects, plants, algae, bacteria, diatoms, and fungi. They have remarkably divergent sequences and structures consistent with their evolution from different progenitors on various occasions; and yet they all bind to ice and inhibit its growth by the adsorption-inhibition mechanism[8]. The AFPs each have a specific surface that acts as its ice-binding site (IBS). These have typically been identified by site-directed mutagenesis of surface residues[9-11]. The IBS is hypothesized to arrange water molecules in an ice-like pattern that matches specific planes of ice. Thus the AFP forms its ligand before binding to it[5, 12]. Ice planes can be defined by their Miller indices, and different AFPs can bind to different planes. Thus, type I AFP from winter flounder binds to the 20-21 pyramidal planes[13], type III AFP binds both primary prism and pyramidal planes using a compound ice-binding surface[11,14], while the spruce budworm AFP, a hyperactive AFP, binds simultaneously to both the primary and basal planes[15,16]. Other hyperactive AFPs, such as *Mp*AFP, bind to multiple ice planes as shown by their complete coverage of single ice crystal hemispheres[5,17]. It is hypothesized, that the ability of hyperactive AFPs to bind the basal plane, as well as other planes, may account for their 10-fold higher activity over moderately active AFPs[18]. Though the efficiency of hyperactive AFPs is well documented, their ability to bind to multiple ice planes is still not understood.

The original method for determining the AFP-bound ice planes was developed by Charles Knight[13,19]. In this method, a macroscopic single ice crystal is mounted onto a hollow metal rod (cold finger) and formed into a hemisphere by submerging it into a hemispherical cup filled with degassed water. Then, the hemisphere is submerged into a dilute solution of AFPs and a layer of ice is grown from the AFP solution onto the ice

crystal hemisphere over several hours controlled by the temperature of the ethylene glycol circulating through the cold finger. The ice crystal is removed from the solution, detached from the cold finger, and placed in a -10 to -15 °C freezer room. The surface is scraped with a sharp blade to remove the frozen surface film of antifreeze protein solution and the ice crystal is allowed to sublimate for at least 3 hr. After sublimation, the ice planes bound by AFPs can be seen as white etched patterns derived from residual protein. The ice hemisphere can be oriented to its *c*-axis and *a*-axes, to locate the basal and prism planes of ice, and determine the Miller indices of the etched patches.

Here we describe a modification of the original method for determining AFP-bound planes of ice, a method we refer to as fluorescence-based ice plane affinity (FIPA)[11]. The AFPs are fluorescently labeled with either a chimeric tag, such as green fluorescent protein (GFP)[11,16,17,20], or with a fluorescent dye covalently bound to the AFP[5,21]. The fluorescently labeled AFPs are adsorbed to a single ice crystal and overgrown using the same experimental procedure as the original ice-etching experiments. The extent of AFP binding to the growing ice hemisphere can be monitored throughout the experiment using an ultraviolet (UV) lamp. After the experiment is complete, the hemisphere can be directly taken off of the cold finger and imaged, without sublimation. However, if desired, the hemisphere can be left to sublimate to visualize a traditional ice etch. Modifications introduced to the FIPA methodology shorten the traditional ice-etching protocol by several hours. Additionally, there is the potential for simultaneously imaging several AFPs, each with a different fluorescent label, to visualize the overlapping patterns of AFP-bound ice planes.

Protocol

1. Growing Single Ice Crystals

1. Take a clean metal pan (15 cm diameter, 4.5 cm high) that fits into, and can float on, an ethylene glycol cooling bath.
2. Prepare polyvinyl chloride (PVC) cylindrical molds, (4.5 cm diameter, 3-4 cm high, 4 mm thick), by sawing sections from a pipe.
    1. Cut a notch, (1 mm wide, 2 mm high) on one side **(Figure 1A)**.
    2. Prepare as many molds that can fit comfortably into the pan **(Figure 1B)**.

    Note: A study showed that polyvinyl alcohol (PVA) can affect ice nucleation[22]. However, in our open mold PVC system we have not encountered problems of atypical ice formation.

3. Apply a light film of vacuum grease to the bottom surface ring of each mold, which is the surface with the notch cut out. Seal this greased, notched surface onto a metal pan with the notches oriented away from the center of the pan. Be careful not to fill or obstruct the notches with grease.
4. Add 0.22 µm filtered and degassed/deionized water to the center of pan, but outside of the molds, and allow the water to slowly enter into the molds through the notches. Be careful not to introduce any bubbles. The water layer should be approximately 5 mm deep.
5. Place the pan into a temperature-controlled ethylene glycol bath cooled to -0.5 °C. The pan should be perfectly level. Add ballast weights to the sides of the pan if necessary.
6. After the pan and water have reached -0.5 °C, add a small piece of ice to the middle of the pan, outside of the molds.
    1. This will nucleate ice growth in the supercooled water across the pan and into the molds. The small notch at the bottom of each mold allows only one ice crystal to propagate through, resulting in a single ice crystal in each mold.
    2. Incubate overnight to form a layer of ice.
7. Over the next three days add 13 ml of 4 °C degassed/deionized water to each mold once a day and drop the temperature of the ethylene glycol bath after each addition to -0.8 °C on day one, to -1.1 °C on day two, and to -1.5 °C on day three.
    1. Incubate at those temperatures overnight.
    2. By day four, the molds should be completely filled with ice.
8. Pull the molds off the pan, push the ice crystals out of the molds, and store on a clean surface, such as a weighing boat, in a -20 °C freezer for approximately 1 hr before handling.
9. Rather than preparing many small single ice crystals, a large single ice crystal several liters in volume can be prepared in a constant temperature incubator as described by Knight[23]. The large ice crystal can be stored for a year or more if kept covered in a -15 to -20 °C freezer. Portions of single crystal can be cut from the ice block with a saw as required.

2. Determining Singularity and Orientation of the Ice Crystal

1. Determine if the ice expelled from the mold is a single crystal by observing in a freezer room, between two crossed polaroids **(Figure 1D)**.
    1. If the ice crystal is single, then no cracks or discontinuities should be seen, and the light direction should not change within the ice crystal.

    Note: If a freezer room is not available, a cold room can be used instead in all required steps, being cautious to work quickly and handle the ice sparingly.

2. Due to the ice birefringence, one may determine orientation of the *c*-axis at the same time. Use the following information to determine the orientation:
    1. When the *c*-axis is exactly parallel to the incident light, in theory, no light will pass through the crossed polaroids. If the incident light is titled slightly from parallel with the *c*-axis, a uniform multicolor spectrum of light is transmitted through the crystal when it is rotated between the crossed polaroids. This uniform transmittance arises from the optical inactivity of ice I_h along its *c*-axis[24]. The basal plane of the ice crystal is normal to the *c*-axis.
    2. When the *c*-axis is further from parallel to the incident light and the ice crystal is rotated between the crossed polaroids, the transmitted light will alternate between 0-100% transmittance with every 90° of rotation of the crystal.

3. Most commonly, the *c*-axis will be normal to the circular plane of the cylindrical ice crystal.

3. Determine the orientation of the *a*-axes by ice pitting[25] which is done by wrapping the ice crystal tightly in aluminum foil, poking a small hole with a needle through the foil into the ice on the basal plane (normal to the *c*-axis), and placing it under vacuum for 20 min.
    1. This treatment will produce an etch with hexagonal symmetry on the basal plane, where the *a*-axes run through the vertices of the six-sided star **(Figure 2A)**.
    2. If desired, the ice crystal can be cut with a saw either parallel or perpendicular to one side of the hexagon to mount it with a primary or secondary prism plane perpendicular to the cold finger, respectively **(Figure 3)**.

3. Adsorption of Fluorescently Labeled Antifreeze Proteins to a Single Ice Crystal

1. Mount a single ice crystal onto the cold finger **(Figure 1C)** by first boring a cavity into the top of the crystal. To do this, alternate melting the ice with a two aluminum rods of slightly different diameter, but similar to the diameter of the cold finger, to form the cavity into which the cold finger can fit.
2. Cool the cold finger to -0.5 °C, place in the ice cavity, and hold the ice crystal in place until it freezes to the metal **(Figure 2B)**. Avoid air bubbles when attaching the crystal to the finger as they hinder efficient transfer of heat from the finger to the rod.
3. Fill a hemispherical cup that is approximately twice the diameter of the ice crystal with filtered deionized water or buffer, cooled to approximately 4 °C. Submerge the cold finger-bound ice crystal into the cup and remove excess water or buffer such that the top of the ice crystal is approximately level with the liquid layer and the ice is not touching the cup walls.
    1. Cover the cup with insulation and lower the temperature to -5 °C.
    2. Wait approximately 1 hr for the ice crystal to form into a hemisphere, checking its status approximately every 20 min **(Figure 2C)**.
    3. The ice will take the shape of the hemispherical cup by melting and growing the ice crystal, but it should never overgrow to touch the cup walls. There should be at least a 1 cm gap between the wall and hemisphere and the cold finger should not protrude from the ice.

4. Remove the cup from the ice crystal and add the fluorescent protein solution to a final volume of 25-30 ml and desired analysis concentration, being careful to keep the total liquid volume in the cup unchanged. A typical AFP concentration is 0.1 mg/ml.
    1. Resubmerge the ice crystal into the cup so that the top of the ice crystal is at level with the liquid and the ice crystal is not touching the cup walls **(Figure 2D)**.
    2. Drop the cold finger temperature to -8 °C and let the protein solution freeze into the ice crystal for 2-3 hr, stirring the solution often. The ice formed from the protein solution should be at least 5 mm before stopping ice growth.

5. Remove the ice crystal from the cup while still attached to the cold finger. Detach the ice from the latter by warming the coolant through the cold finger to just above 0 °C and wait until the ice crystal melts off.
6. Place the crystal flat side down onto a clean surface, such as a weighing dish, being careful not to touch the newly form ice and store at -20 °C for at least 20 min before handing.

4. Visualization of Antifreeze-protein-bound Planes of Ice

1. Visualization of fluorescence is done in a darkened freezer or cold room, by placing the ice crystal flat side down under lamps with wavelength specific excitation filters to excite the fluorescent label and camera emission filters to block out any other nonspecific light. Based on the pattern, the ice planes that are bound by AFPs can be estimated **(Figure 4)**.
2. If wavelength specific lights are not available a UV light box can be used instead.
3. Traditional ice etches can also be performed simply by allowing the ice hemisphere to sublimate at -20 °C for at least 3 hr, after which residual protein powder may become visible on the ice surface **(Figure 5)**.
4. Step 2.3 can be repeated in order to determine the orientation of the *a*-axes of the completed ice hemisphere.

Representative Results

Preparation and mounting of the single ice crystal are the two steps of the FIPA procedure where errors are most commonly made. Determining if the prepared ice crystal is single is done by examining it through crossed polaroids **(Figure 1D)**, as outlined in step 2.1 of the protocol section. If a multicrystalline ice crystal is used for the FIPA analysis, the result will be discontinuous binding of the AFPs on the hemisphere without a coherent binding pattern **(Figure 6B)**. If the ice crystal interfaces are located around the ice planes to which the AFP binds the final result may not be interpretable. For this reason, the ice crystal should be carefully checked for singularity before moving onto the next steps. To increase the probability of having single ice crystals for the FIPA analysis several should be made at the same time.

Another common error is incorrectly aligning the crystal faces with the cold finger during mounting. To mount the primary or secondary prism faces perpendicular to the cold finger, the single ice crystal must first be oriented by ice pitting, then cut based on the orientation of the star-shaped etch **(Figures 2A** and **3)**, as outlined in step 2.3 of the protocol section. If the ice crystal is mounted misaligned the final result will produce a hemisphere where the equator of the hemisphere does not align with the symmetry of the ice planes **(Figure 6C)**. Although this is an interpretable result, it will be less informative than a correctly aligned ice crystal since the largest circumference of the hemisphere is at the equator **(Figure 4)**.

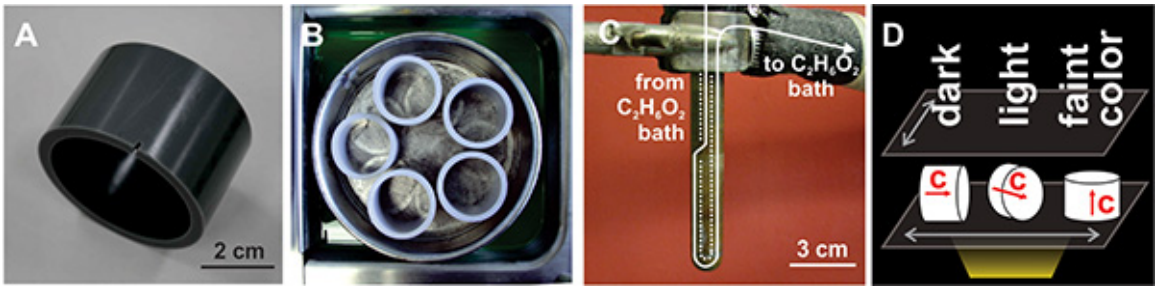

Figure 1. Equipment for growing and mounting single ice crystals. A) PVC molds. **B**) Pan in ethylene glycol bath with PVC molds. **C**) Cold finger with flow of ethylene glycol shown by the white arrow. The white dashed line indicates the inner wall of the cold finger. **D**) Diagram of crossed polaroids for orienting a single ice crystal. The light source is yellow, crossed polaroids are grey and the single ice crystal is white. The orientation of the polaroids (gray arrows) and ice crystal orientation (red arrows) are indicated. From left to right the ice crystal is oriented such that the *c*-axis is perpendicular to the bottom polaroid, 45° to the bottom polaroid, and parallel to the incident light. The light passing though the crossed polaroids and ice will appear dark, light, or faintly multicolored through the top polaroid depending on the orientation of the ice crystal. Click here to view larger image.

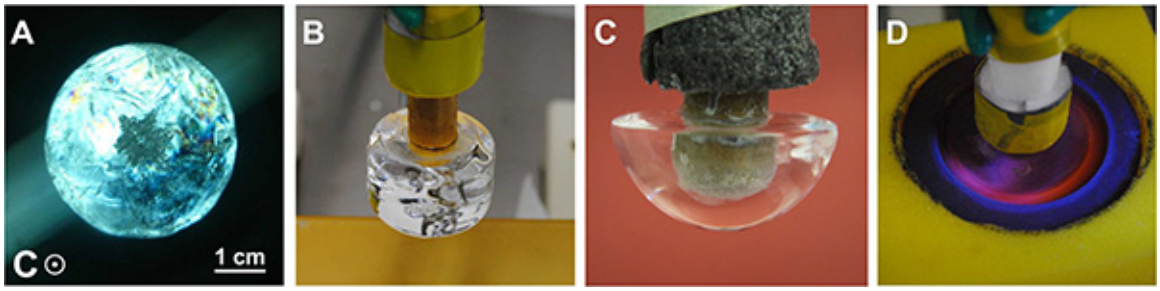

Figure 2. Preparing ice crystal for FIPA. A) Determining axes orientations by ice etch with hexagonal symmetry. The basal plane of the crystal is parallel to the plane of the page. **B**) Mounting the single ice crystal onto the cold finger. **C**) Ice after forming into hemisphere. **D**) Ice hemisphere submerged in hemispherical cup filled with protein solution. Click here to view larger image.

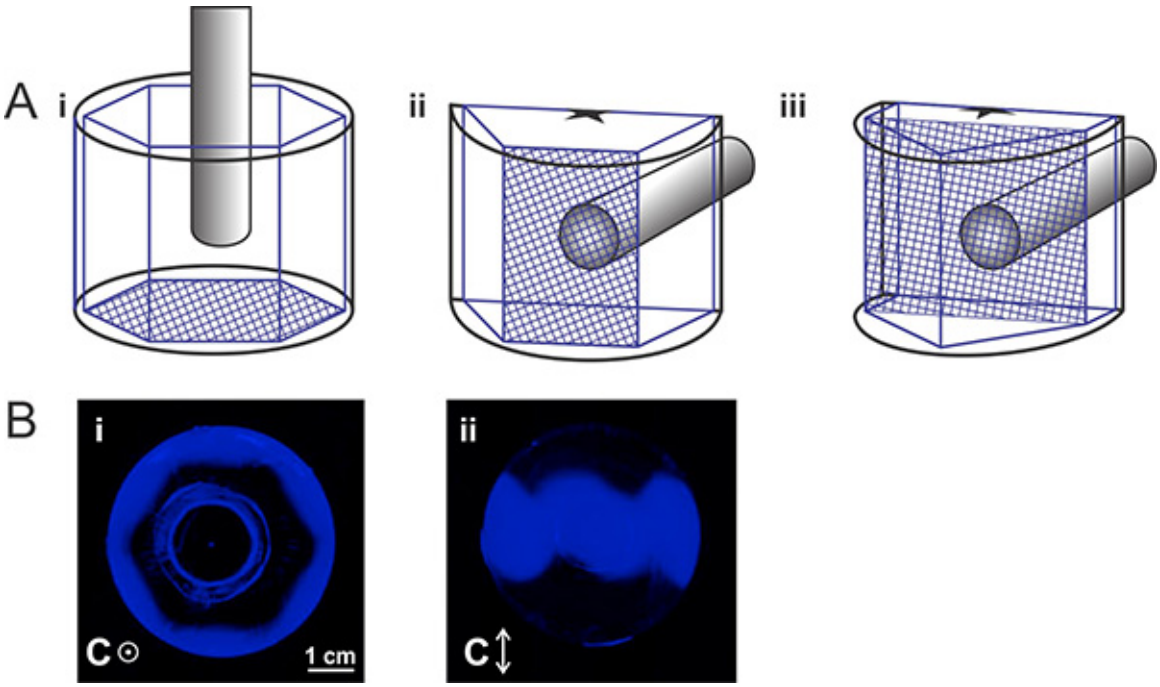

Figure 3. Mounting ice crystal based on orientation. A) Diagram of mounting ice with (i) the basal plane, (ii) a primary prism plane, and (iii) a secondary prism plane perpendicular to the cold finger. For orientations (ii) and (iii) the ice crystal must be cut in half, as shown in the figure. **B**) FIPA results of Pacific blue-labeled type III nfeAFP8 after mounting ice crystals with (i) the basal plane and (ii) a primary prism plane perpendicular to the cold finger. Click here to view larger image.

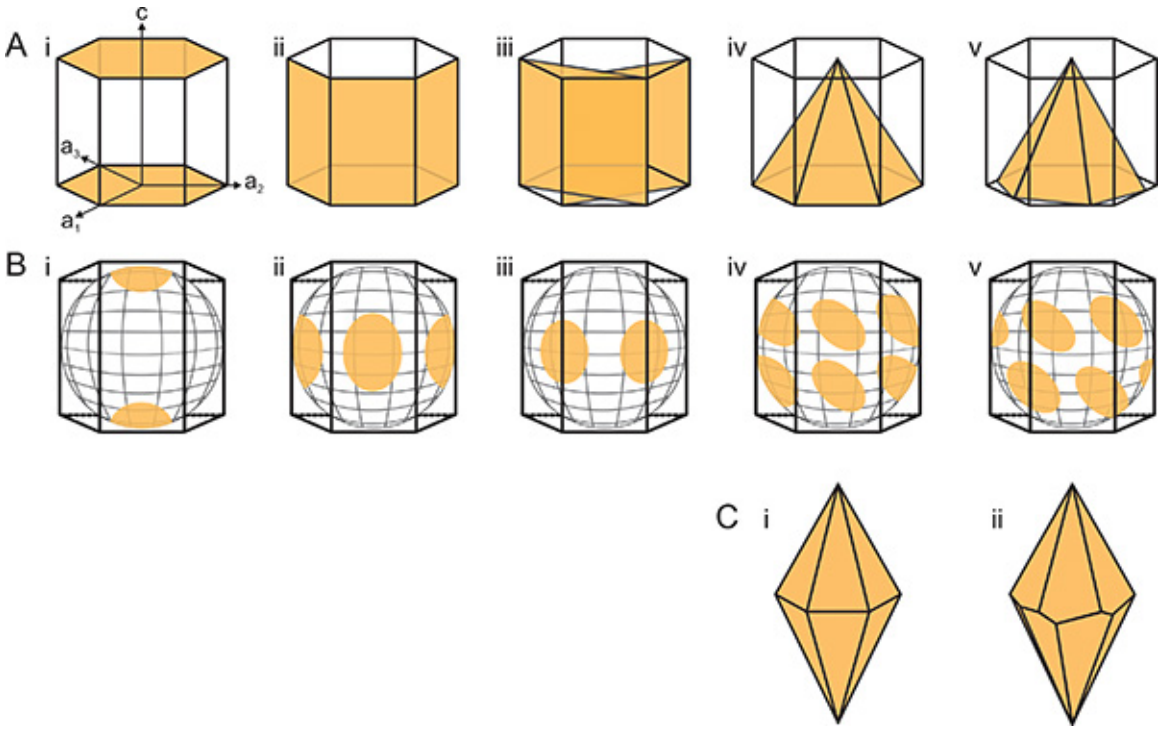

Figure 4. Interpreting AFP-bound planes from FIPA analysis results. A) Representation of the bound planes of I_h ice; and **B**) the corresponding FIPA analysis result when the single ice crystal is mounted with a primary prism plane perpendicular to the cold finger. Panels represent (i) basal plane, (ii) primary prism plane, (iii) secondary prism plane, (iv) pyramidal plane aligned with the *a*-axes, and (v) pyramidal plane offset to the *a*-axes. **C**) Morphology of a single ice crystal when grown in solution of AFPs that bind pyramidal planes i) aligned to the *a*-axes and ii) offset from the *a*-axes. Click here to view larger image.

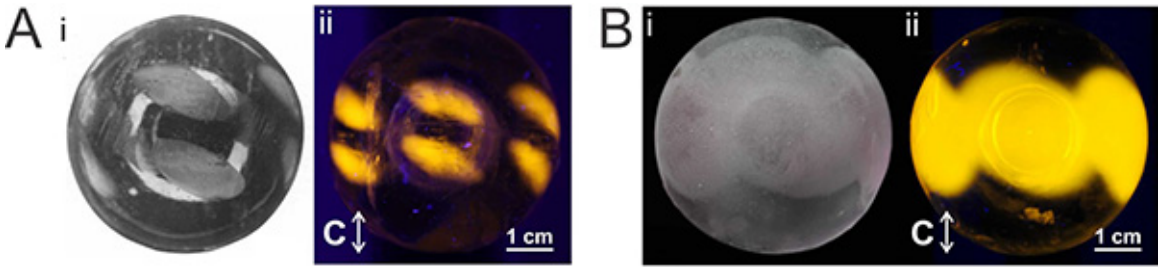

Figure 5. Comparison of traditional ice etches versus FIPA. A) (i) The traditional etch of type I AFP (HPLC6 isoform) produced by the winter flounder (*Pseudopleuronectes americanus*) is shown as originally produced by Knight *et al*., (1991). (ii) The corresponding FIPA analysis of the same protein labeled with TRITC. **B**) (i) Traditional etch of a quadruple IBS mutant (V9Q/V19L/G20V/I41V) of type III nfeAFP11 (from the Japanese eel pout *Zoarces elongatuskner*)[21]. (ii) The corresponding FIPA analysis of the same protein labeled with TRITC. Click here to view larger image.

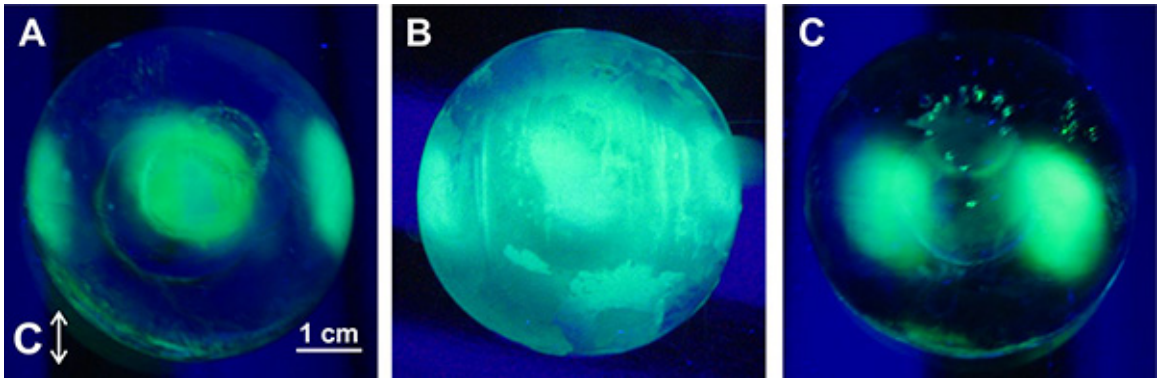

Figure 6. Hemispheres resulting from common FIPA analysis errors. Analyses were conducted on GFP-tagged type III HPLC12-A16H. **A**) An optimal FIPA result for comparison. The ice crystal was mounted with its primary prism plane perpendicular to the cold finger. **B**) FIPA analysis that was inadvertently conducted using an ice hemisphere composed of more than one crystal. **C**) FIPA analysis that was conducted on a misaligned single ice crystal. The secondary prism plane was not mounted exactly perpendicular to the cold finger. Click here to view larger image.

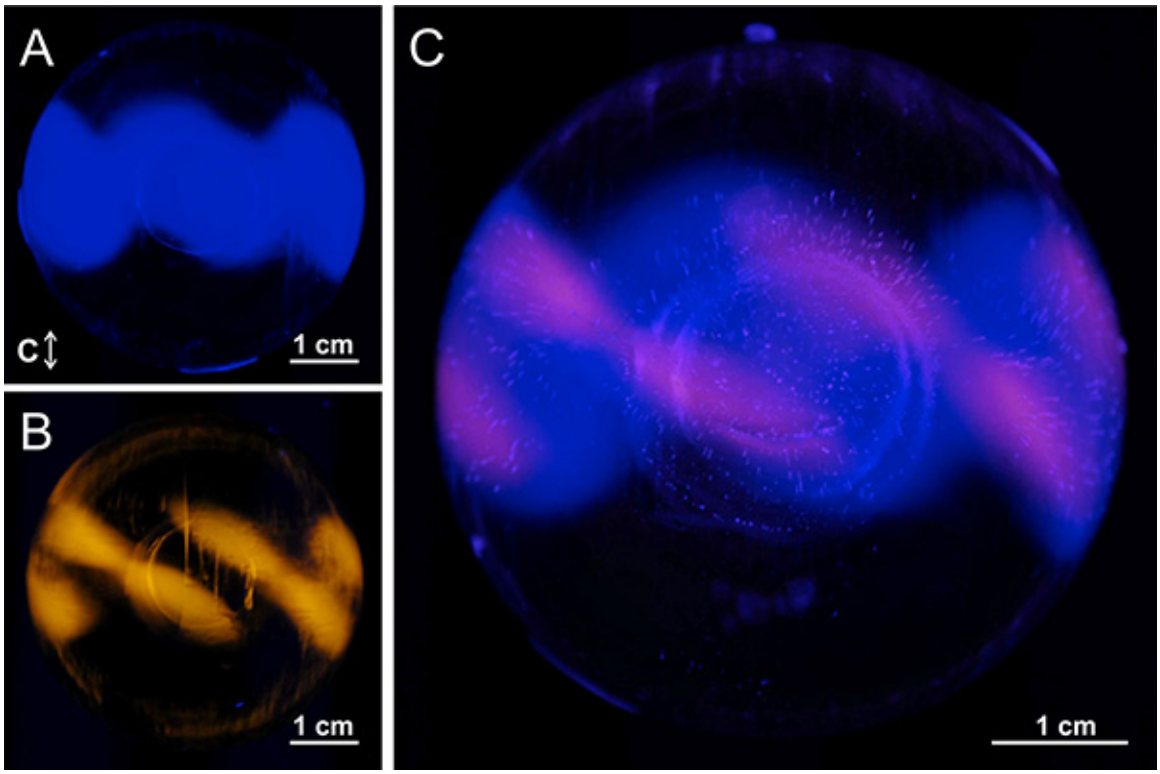

Figure 7. Using FIPA analysis to compare ice-binding patterns of different AFPs. Pacific blue-labeled type III nfeAFP8 was combined with TRITC-labeled type I AFP and a single FIPA analysis was conducted. **A**) Visualization of type III nfeAFP8 only. **B**) Visualization of type I AFP only. **C**) Visualization of type III nfeAFP8 and type I AFP together. Click here to view larger image.

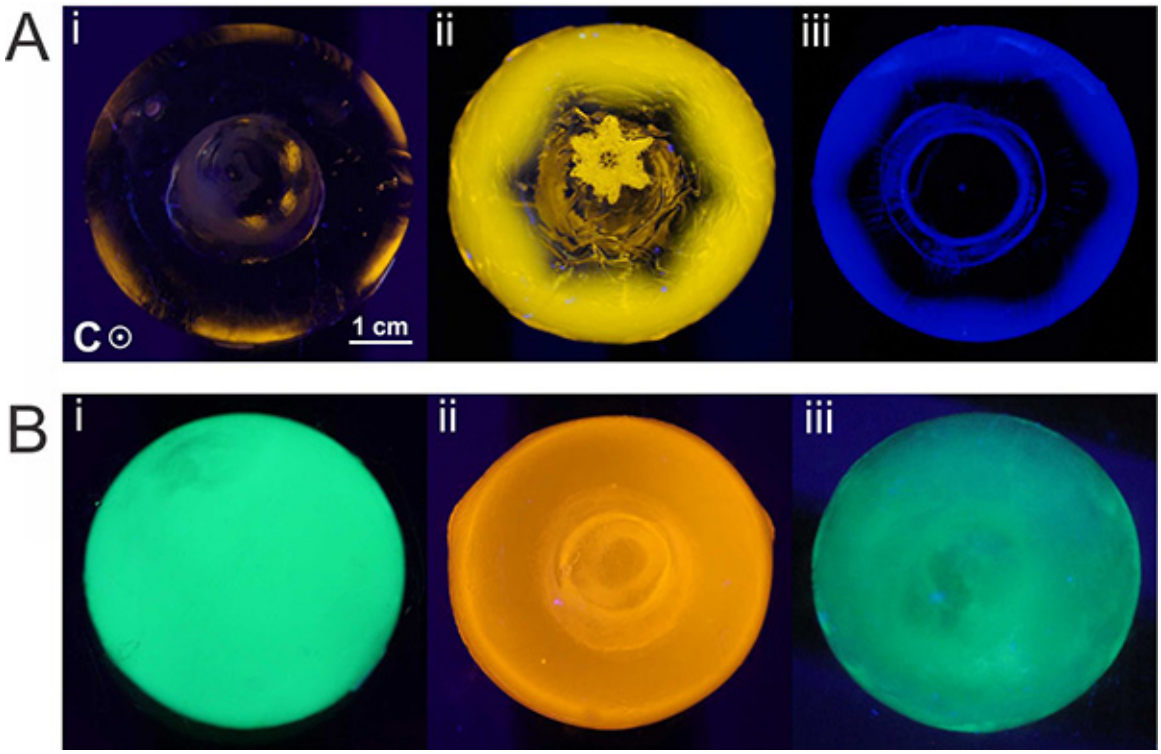

Figure 8. FIPA of moderately active and hyperactive AFPs. A) FIPA analysis of three different moderately active fish AFPs; (i) TRITC-labeled type I AFP (HPLC6 isoform, *Pseudopleuronectes americanus*), (ii) TRITC-labeled type II AFP(Ca^{2+}-independent isoform, *Longsnout poacher)*, (iii) Pacific-blue-labeled type III AFP (nfeAFP8 isoform, *Zoarces elongatuskner*). **B**) FIPA analysis of three different hyperactive AFPs; (i) GFP-tagged *Mp*AFP_RIV (*Marinomonas primoryensis*), (ii) TRITC-labeled sbwAFP (*Choristoneura fumiferana*), (iii) GFP-tagged *Tm*AFP (*Tenebrio molitor*). In all images, the *c*-axis is perpendicular to the plane of the page. Click here to view larger image.

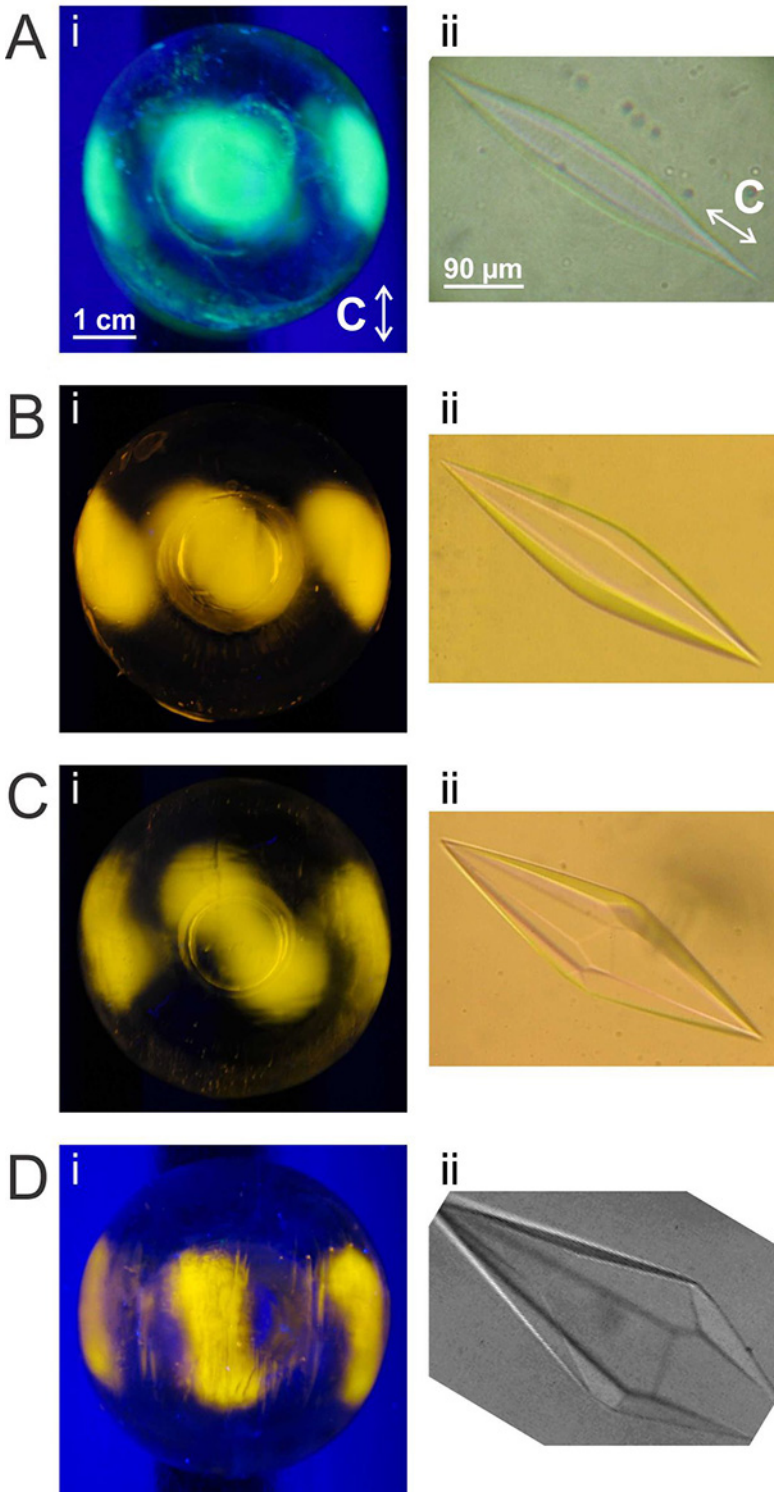

Figure 9. Relation of fluorescent pattern produced by FIPA analysis to ice-crystal morphology of different type III AFP isoforms and mutants[11,21]. **A**) (i) FIPA analysis of GFP-tagged QAE-A16H. (ii) Ice crystal morphology produced by QAE-A16H. **B**) (i) FIPA analysis of TRITC-labeled nfeAFP11-V9Q. (ii) Ice crystal morphology produced by nfeAFP11-V9Q. **C**) (i) FIPA analysis of TRITC-labeled wild-type nfeAFP11. (ii) Ice-crystal morphology produced by wild-type nfeAFP11. **D**) (i) FIPA analysis of TRITC-labeled wild-type nfeAFP6. (ii) Ice-crystal morphology produced by wild-type nfeAFP6. *C*-axis orientations and scale bars are as indicated. Click here to view larger image.

Discussion

Development of the ice-etching method by Charles Knight for determination of AFP-bound ice planes greatly advanced studies on the mechanism of ice binding by AFPs. Whereas structures of AFPs could be solved by X-ray crystallography[26,27] there was no obvious method for deducing the complementary surface on ice to which the AFP bound. When type I AFP from winter flounder was initially characterized, it was hypothesized to bind to the primary prism planes of ice[28]. However, Knight's ground breaking ice-etching experiments of type I AFP showed that they bind to pyramidal planes of ice[13]. This result stimulated the AFP research community to rethink the mechanism of AFP ice binding and more accurately determine the ice-binding face of AFPs[9]. Knight's original ice-etching experiments were done using native AFPs purified from the AFP-producing organisms. With the development of recombinant AFPs and the increasing use of GFP tags, there was an opportunity to expand these studies to many other AFPs[29].

The idea of incorporating covalent fluorescent protein dyes, such as tetramethylrhodamine-5-(and 6)-isothiocyanate (TRITC), into the analysis came only after the success of the GFP-fused AFP FIPA analyses[11]. The chimeric fluorescent protein tags and the chemical modifications by covalent dyes have been observed not to affect the ice-binding patterns of the AFPs **(Figure 5)**.With the former, GFP is fused to either the N- or C- terminal ends of the AFPs, which are often well removed from the IBS. Also, a flexible linker can be inserted between the GFP and AFP allowing the tag to be pushed away from the ice surface. With the latter labeling strategy, the charged side chains that react with the covalent dyes are usually on surfaces away from the IBS. If the strategies presented here for fluorescently labeling AFPs do not work, introduction of a cysteine away from the IBS for reaction with thiol-reactive dyes is another option[30]. By taking measures to ensure the fluorescent labels do not affect AFP ice binding, as judged by thermal hysteresis activity and ice crystal morphology, we are confident that the FIPA analysis shows true representation of AFP ice-binding patterns, as it did in the original ice-etching method.

There are several benefits to fluorescently labeling the AFPs for the FIPA analysis. Less time is required for the procedure since the sublimation of ice for visualization of AFP-bound planes is not needed. The incorporation of labeled protein into the hemisphere can be monitored during the growth of the ice to assess experimental completion and the AFP-binding pattern can be recorded at any point. This prevents unnecessarily long experiments, or premature completion of ice growth. The fluorescent labeling allows clearer AFP-binding pattern visualization than previously possible with etching, as is seen in the comparison of results from both methods applied to type I and type III AFPs **(Figure 5)**. However, a post-FIPA ice-etch can be easily conducted by placing the hemisphere in a freezer for several hours, meaning that both analyses can be done on the same sample since similar AFP concentrations are needed for both methods. A valuable advantage of FIPA is the ability to visualize more than one differently-labeled AFP on the same ice hemisphere **(Figure 7)**. This is useful for illustrating differences in AFP ice-binding planes seen with different AFP types, isoforms, and activity mutants.

FIPA analysis has already been used in several AFP studies. It has been used to support the hypothesis that basal plane binding is unique to hyperactive AFPs and necessary for their high activity[18]. Moderately active AFPs were found not to bind the basal plane **(Figure 8A)** but many hyperactive AFPs completely cover the ice hemisphere, including the basal plane of ice **(Figure 8B)**[5,20,31]. FIPA analysis has also been used to study the function of specific ice-binding residues. For example, FIPA analysis was conducted on several type III isoforms and mutants, some of which prevent ice growth, and some of which have been found to only shape ice[11,21,32]. From the studies, it was found that particular residues are important in incorporation of the AFPs into ice and others are important in ice plane specificity **(Figure 9)**.

Other methods for studying AFP-binding patterns on single ice crystals include direct observation by fluorescence microscopy[16,33] and microfluidics[34]. These methods have the advantage of sensitivity to the dynamic of the attachment of the AFP to ice and monitoring of ice shaping simultaneity with the affinity of the AFP to the ice, but are less robust compare to the FIPA method in determining the affinity to the ice planes. Molecular dynamics is also being used to predict the ice-plane binding specificity of AFPs[12,20,21,30,35]. Using FIPA analysis, along with the other available techniques, we are learning the ice-plane binding patterns of each AFPs, the importance of the composition of the IBS in selecting ice planes, and how binding of specific planes is related to AFP activity.

Disclosures

No conflicts of interest declared.

Acknowledgements

PLD holds the Canada Research Chair in Protein Engineering. This work was funded by a grant from the Canadian Institutes of Health Research to PLD. This work was also supported by a Grant-in-Aid for scientific research from the Japan Society for the Promotion of Science (JSPS) (No. 23310171) and from the Japan Bio-oriented Technology Research Advancement Institution (BRAIN). We are grateful to Drs. Chris Marshall and Mike Kuiper for pioneering work that led to FIPA. We are also grateful to Dr. Sakae Tsuda for providing facilities for some of this work and to Dr. Laurie Graham for setting up the fluorescent light excitation and emission filters.

References

1. Devries, A.L. Antifreeze peptides and glycopeptides in cold-water fishes. *Annu. Rev. Physiol.* **45,** 245-60 (1983).
2. Sidebottom, C., *et al.* Phytochemistry - heat-stable antifreeze protein from grass. *Nature.* **406** (6793), 256-256 (2000).
3. Tomczak, M.M., *et al.* A mechanism for stabilization of membranes at low temperatures by an antifreeze protein. *Biophys. J.* **82** (2), 874-81 (2002).
4. Gilbert, J.A., Davies, P.L., and Laybourn-Parry, J.A. Hyperactive, Ca^{2+}-dependent antifreeze protein in an antarctic bacterium. *FEMS Microbiol. Lett.* **245** (1), 67-72 (2005).

5. Garnham, C.P., Campbell, R.L., and Davies, P.L. Anchored clathrate waters bind antifreeze proteins to ice. *Proc. Natl. Acad. Sci. U.S.A.* **108** (18), 7363-7367 (2011).
6. Guo, S., Garnham, C.P., Whitney, J.C., Graham, L.A., and Davies, P.L. Re-evaluation of a bacterial antifreeze protein as an adhesin with ice-binding activity. *Plos One.* **7** (11), e48805 (2012).
7. Raymond, J.A. Algal ice-binding proteins change the structure of sea ice. *Proc. Natl. Acad. Sci. U.S.A.* **108** (24), E198-E198 (2011).
8. Raymond, J.A. and Devries, A.L. Adsorption inhibition as a mechanism of freezing resistance in polar fishes. *Proc. Natl. Acad. Sci. U.S.A.* **74** (6), 2589-2593 (1977).
9. Baardsnes, J.*, et al.* New ice-binding face for type i antifreeze protein. *FEBS Lett.* **463** (1-2), 87-91 (1999).
10. Middleton, A.J., Brown, A.M., Davies, P.L., and Walker, V.K. Identification of the ice-binding face of a plant antifreeze protein. *FEBS Lett.* **583** (4), 815-819 (2009).
11. Garnham, C.P.*, et al.* Compound ice-binding site of an antifreeze protein revealed by mutagenesis and fluorescent tagging. *Biochemistry.* **49** (42), 9063-9071 (2010).
12. Nutt, D.R. and Smith, J.C. Dual function of the hydration layer around an antifreeze protein revealed by atomistic molecular dynamics simulations. *J. Am. Chem. Soc.* **130** (39), 13066-73 (2008).
13. Knight, C.A., Cheng, C.C., and Devries, A.L. Adsorption of alpha-helical antifreeze peptides on specific ice crystal-surface planes. *Biophys. J.* **59** (2), 409-418 (1991).
14. Antson, A.A.*, et al.* Understanding the mechanism of ice binding by type iii antifreeze proteins. *J. Mol. Biol.* **305** (4), 875-89 (2001).
15. Graether, S.P.*, et al.* Beta-helix structure and ice-binding properties of a hyperactive antifreeze protein from an insect. *Nature.* **406** (6793), 325-328 (2000).
16. Pertaya, N., Marshall, C.B., Celik, Y., Davies, P.L., and Braslavsky, I. Direct visualization of spruce budworm antifreeze protein interacting with ice crystals: Basal plane affinity confers hyperactivity. *Biophys. J.* **95** (1), 333-341 (2008).
17. Middleton, A.J.*, et al.* Antifreeze protein from freeze-tolerant grass has a beta-roll fold with an irregularly structured ice-binding site. *J. Mol. Biol.* **416** (5), 713-724 (2012).
18. Scotter, A.J.*, et al.* The basis for hyperactivity of antifreeze proteins. *Cryobiology.* **53** (2), 229-239 (2006).
19. Knight, C.A., Wierzbicki, A., Laursen, R.A., and Zhang, W. Adsorption of biomolecules to ice and their effects upon ice growth. 1. Measuring adsorption orientations and initial results. *Crys. Growth Des.* **1** (6), 429-438 (2001).
20. Hakim, A.*, et al.* Crystal structure of an insect antifreeze protein and its implications for ice binding. *J. Biol. Chem.* **288** (17), 12295-304 (2013).
21. Garnham, C.P., Nishimiya, Y., Tsuda, S., and Davies, P.L. Engineering a naturally inactive isoform of type iii antifreeze protein into one that can stop the growth of ice. *FEBS Lett.* **586** (21), 3876-3881 (2012).
22. Holt, C.B. The effect of antifreeze proteins and poly(vinyl alcohol) on the nucleation of ice: A preliminary study. *Cryo Letters.* **24** (5), 323-30 (2003).
23. Knight, C.A. A simple technique for growing large, optically "perfect" ice crystals. *J. Glac.* **42** (142), 585-587 (1996).
24. Hobbs, P.V., *Ice physics*. Oxford: Clarendon Press. 200-248 (1974).
25. Knight, C. Formation of crystallographic etch pits on ice, and its application to the study of hailstones. *J. Appl. Meteorol.* **5** (5), 710-714 (1966).
26. Yang, D.S., Sax, M., Chakrabartty, A., and Hew, C.L. Crystal structure of an antifreeze polypeptide and its mechanistic implications. *Nature.* **333** (6170), 232-7 (1988).
27. Sicheri, F. and Yang, D.S. Ice-binding structure and mechanism of an antifreeze protein from winter flounder. *Nature.* **375** (6530), 427-31 (1995).
28. Devries, A.L. Role of glycopeptides and peptides in inhibition of crystallization of water in polar fishes. *Philos. T Roy. Soc. B.* **304** (1121), 575-588 (1984).
29. Pertaya, N.*, et al.* Fluorescence microscopy evidence for quasi-permanent attachment of antifreeze proteins to ice surfaces. *Biophys. J.* **92** (10), 3663-3673 (2007).
30. Kondo, H.*, et al.* Ice-binding site of snow mold fungus antifreeze protein deviates from structural regularity and high conservation. *Proc. Natl. Acad. Sci. U.S.A.* **109** (24), 9360-9365 (2012).
31. Mok, Y.F.*, et al.* Structural basis for the superior activity of the large isoform of snow flea antifreeze protein. *Biochemistry.* **49** (11), 2593-2603 (2010).
32. Takamichi, M., Nishimiya, Y., Miura, A., and Tsuda, S. Fully active qae isoform confers thermal hysteresis activity on a defective sp isoform of type iii antifreeze protein. *FEBS J.* **276** (5), 1471-1479 (2009).
33. Bar-Dolev, M., Celik, Y., Wettlaufer, J.S., Davies, P.L., and Braslavsky, I. New insights into ice growth and melting modifications by antifreeze proteins. *J. R. Soc. Interface.* **9** (77), 3249-3259 (2012).
34. Celik, Y.*, et al.* Microfluidic experiments reveal that antifreeze proteins bound to ice crystals suffice to prevent their growth. *Proc. Natl. Acad. Sci. U.S.A.* **110** (4), 1309-1314 (2013).
35. Garnham, C.P., Campbell, R.L., Walker, V.K., and Davies, P.L. Novel dimeric beta-helical model of an ice nucleation protein with bridged active sites. *BMC Struct. Biol.* **11,** (2011).

